*J. Mater. Environ. Sci. 7 (10) (2016) 3895-3905*
*ISSN : 2028-2508*
*CODEN: JMESCN*



# Physicochemical Characterization and Corrosion Inhibition Potential of 4, 5-(alkylthio)-1, 3-dithiole-2-thione for mild steel in 1 M hydrochloric acid

**D. Jeroundi[1], H. Elmsellem[2*], S. Chakroune[1], B. Hammouti[2], R. Idouhli[3], E. M. El Hadrami[1], A. Ben-Tama[1], M. Oudani[4], Y. Ouzidan[1] and Y. Kandri Rodi[1]**

[1]*Laboratoire de Chimie Organique Appliquée, Université Sidi Mohamed Ben Abdellah, Faculté des Sciences et Techniques, Route d'Immouzzer, BP 2202, Fès, Morocco.*

[2] *Laboratoire de chimie analytique appliquée, matériaux et environnement (LC2AME), Faculté des Sciences, B.P. 717, 60000 Oujda, Morocco.*

[3]*Laboratory of Physical Chemistry of Materials and Environment, Department of Chemistry, University Cadi Ayyad, Faculty of Science Semlalia, BP 2390 Marrakech, Morocco.*

[4]*Laboratoire de Modélisation et Calcul Scientifique, Université Sidi Mohamed Ben Abdellah, Fès, Maroc*

*Received 22 May 2016, Revised 29 Jul 2016, Accepted 5 Aug 2016*
**Corresponding author. E-mail: h.elmsellem@yahoo.fr, Tél : +212670923431*

## Abstract

Present study describes the inhibition property of 4, 5- (alkylthio) - 1, 3- dithiole- 2- thione(P2) on mild steel corrosion in 1 M HCl using weight loss, electrochemical, and DFT. Results showed that the corrosion inhibition efficiency (E%) increases with increasing P2 concentration and attained the maximum value of 89% at $10^{-3}$ M concentration. Polarization studies revealed that P2 acted as mixed-type inhibitor. Electrochemical impedance spectroscopy (EIS) studies suggested that the P2 inhibits mild steel corrosion by becoming adsorbate at the metallic/electrolyte surfaces. Among the several tested isotherms, adsorption of the P2 on mild steel surface obeyed the Langmuir adsorption isotherm. Quantum chemical parameters are calculated using the density functional theory (DFT) method. Correlation between theoretical and experimental results is discussed.

*Keywords:* Mild steel,1,3- dithiole, TTF, EIS, Corrosion, Weight loss, EIS, DFT.

## 1. Introduction

The synthesis and the characterization of new heterocyclic systems based on sulfur has been one of the central objective in contemporary organic chemistry. This review deals with the interesting and diverse chemistry of 1,3- dithiole- 2- thione-4,5- dithiolate [1], which is the key compound for the preparation of tetrathiafulvalene (TTF) and its derivatives, well-known for their π- electron- donating abilities and two reversible oxidation processes. TTF and related heterocycles have received [2- 6] much interest over the past forty years. Since the discovery of the first metallic charge transfer salts based on TTF [7] , a great number of TTF derivatives have been synthesized and investigated, such as tetrathiaflvalenylallene [8], TTF oligomers [9-10] and π- extended TTF derivatives [11]. They have been extensively studied for various applications, such as sensors, receptors, switches, conductors [12-18] and in the field of conducting organic materials involving intermolecular charge transfer interactions with various π- accepting molecules [19-20]. This work presents new properties of fragment of TTF by testing 4, 5- (alkylthio) - 1, 3- dithiole- 2- thione on the corrosion.

## 2. Experimental

### *2.1. Synthesis of inhibitor*

To a solution of zinc complex (5.3mmol) in 50 ml of acetone was added 2- chloroethan-1- ol (37.1mmol). The mixture was heated to reflux under nitrogen for 2 days. After the reaction was cooled down and filtered, the product is obtained as a yellow gold powder (**Scheme 1**):

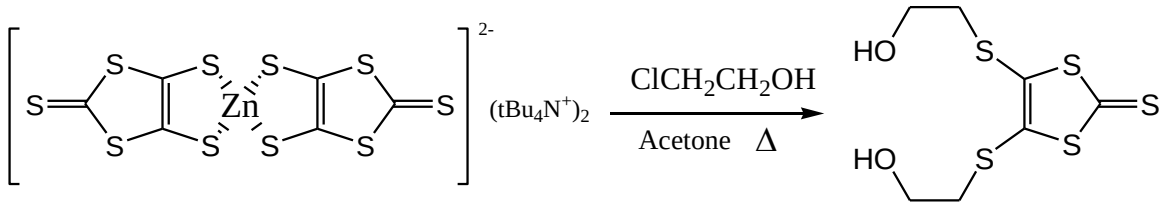


**Scheme 1:**Synthesis of 4, 5- (alkylthio) - 1, 3- dithiole- 2- thione (**P2**).

The analytical and spectroscopic data are conforming to the structure of compounds formed:
**(P2): Yield:** 74%; **MP:** 70°C; **RMN $^{1}$H ($CDCl_3$) (δ ppm):** 3, 09(4H, t, $SCH_2$, J= 5, 6Hz); 3, 85(4H, m, $CH_2OH$); **RMN $^{13}$C ($CDCl_3$) (δ ppm):**33, 4 ($SCH_2$); 61 ($CH_2OH$); 125 (C=C); 208 (C=S).

*2.2. Materials*
The steel used in this study is a mild steel with a chemical composition 0.09 wt. % P; 0.38 wt. % Si; 0.01 wt. % Al; 0.05 wt. % Mn; 0.21 wt. % C; 0.05 wt. % S and the remainder iron (Fe).

*2.2.1. Preparation of Solutions*
The aggressive solutions of 1.0 M HCl were prepared by dilution of analytical grade 37% HCl with distilled water. Inhibitor were dissolved in acid solution at the required concentrations (in mol/l) (volume of inhibitor/volume of HCl), and the solution in the absence of inhibitor was taken as blank for comparison purposes. The test solutions were freshly prepared before each experiment by adding P2 to the corrosive solution. The concentrations of P2 were $10^{-3}$ to $10^{-6}$ M.

*2.2.2. Gravimetric Study*
Gravimetric experiments were performed according to the standard methods [21], the carbon steel specimens (1.5 cm × 1.5 cm × 0.05 cm) were abraded with a series of emery papers SiC (120, 600, and 1200 grades) and then washed with distilled water and acetone. After weighing accurately, the specimens were immersed in a 100 mL of 1.0 M HCl solution with and without addition of different concentrations of inhibitor P2.
All the aggressive acid solutions were open to air. After 6 hours of acid immersion, the specimens were taken out, washed, dried, and weighed accurately. In order to get good reproducibility, all measurements were performed few times and average values were reported.
The average weight loss was obtained. The corrosion rate (*v*) is calculated using the following equation:

$$v = \frac{w}{st} (\mathbf{1})$$

Where: W is the average weight loss, S the total area, and t is immersion time. With the corrosion rate calculated, the inhibition efficiency ($E_w$) is determined as follows:

$$Ew\ \% = \frac{V_0 - V}{V_0} X\ 100 \quad (\mathbf{2})$$

Where: $\boldsymbol{v_0}$ and *v* are, respectively, the values of corrosion rate with and without inhibitor.

*2.2.3. Electrochemical Measurements*
The electrochemical measurements were carried out using Volta lab (Tacussel - Radiometer PGZ 100) potentiostat controlled by Tacussel corrosion analysis software model (Voltamaster 4) at static condition. The corrosion cell used had three electrodes. The reference electrode was a saturated calomel electrode (SCE). A platinum electrode was used as auxiliary electrode of surface area of 1 $cm^2$. The working electrode was carbon steel of the surface 1$cm^2$. All potentials given in this study were referred to this reference electrode. The working electrode was immersed in the test solution for 30 minutes to establish a steady state open circuit potential ($E_{ocp}$). After measuring the $E_{ocp}$, the electrochemical measurements were performed. All electrochemical tests have been performed in aerated solutions at 308 K. The EIS experiments were conducted in the frequency range with high limit of 100 kHz and different low limit 0.1 Hz at open circuit potential, with 10 points per decade, at the rest potential, after 30 min of acid immersion, by applying 10 mV ac voltage peak-to-peak. Nyquist plots were made from these experiments. The best semicircle can be fit through the data points in the Nyquist plot using a non-linear least square fit so as to give the intersections with the x-axis.

The inhibition efficiency of the inhibitor was calculated from the charge transfer resistance values using the following equation:

$$E\% = \frac{R_{ct} - R_{ct}^{\circ}}{R_{ct}} x100 \quad \textbf{(3)}$$

Where, $R^{\circ}_{ct}$ and $R_{ct}$ are the charge transfer resistance in absence and in presence of inhibitor, respectively.

*2.3. Quantum chemical calculations*

Quantum chemical calculations are used to correlate experimental data for inhibitors obtained from different techniques (viz., electrochemical and weight loss) and their structural and electronic properties. According to Koopman's theorem [22], $E_{HOMO}$ and $E_{LUMO}$ of the inhibitor molecule are related to the ionization potential (I) and the electron affinity (A), respectively. The ionization potential and the electron affinity are defined as $I = -E_{HOMO}$ and $A = -E_{LUMO}$, respectively. Then absolute electronegativity (χ) and global hardness (η) of the inhibitor molecule are approximated as follows [20]:

$$\chi = \frac{I+A}{2}, \quad \chi = -\frac{1}{2}(E_{HOMO} + E_{LUMO}) \quad \textbf{(4)}$$

$$\eta = \frac{I-A}{2}, \quad \eta = -\frac{1}{2}(E_{HOMO} - E_{LUMO}) \quad \textbf{(5)}$$

Where $I = -E_{HOMO}$ and $A = -E_{LUMO}$ are the ionization potential and electron affinity respectively.

The fraction of transferred electrons ΔN was calculated according to Pearson theory [23]. This parameter evaluates the electronic flow in a reaction of two systems with different electronegativities, in particular case; a metallic surface (Fe) and an inhibitor molecule. ΔN is given as follows:

$$\Delta N = \frac{\chi_{Fe} - \chi_{inh}}{2(\eta_{Fe} + \eta_{inh})} \quad \textbf{(6)}$$

Where χFe and χinh denote the absolute electronegativity of an iron atom (Fe) and the inhibitor molecule, respectively; ηFe and ηinh denote the absolute hardness of Fe atom and the inhibitor molecule, respectively. In order to apply the eq. 6 in the present study, a theoretical value for the electronegativity of bulk iron was used χFe = 7 eV and a global hardness of ηFe = 0, by assuming that for a metallic bulk I = A because they are softer than the neutral metallic atoms [24].

The electrophilicity has been introduced by Sastri et al. [25], is a descriptor of reactivity that allows a quantitative classification of the global electrophilic nature of a compound within a relative scale. They have proposed the ω as a measure of energy lowering owing to maximal electron flow between donor and acceptor and ω is defined as follows.

$$\omega = \frac{\chi^2}{2\eta} \quad \textbf{(7)}$$

The Softness σ is defined as the inverse of the η [23]

$$\sigma = \frac{1}{\eta} \quad \textbf{(8)}$$

Using left and right derivatives with respect to the number of electrons, electrophilic and nucleophilic Fukui functions for a site k in a molecule can be defined [24].

$$f_k^+ = P_k(N+1) - P_k(N) \quad for\ nucleophilic\ attack \quad \textbf{(9)}$$

$$f_k^- = P_k(N) - P_k(N-1) \quad for\ electrphilic\ attack \quad \textbf{(10)}$$

$$f_k^+ = [P_k(N+1) - P_k(N-1)]/2 \quad for\ radical\ attack \quad \textbf{(11)}$$

where, $P_k(N)$, $P_k(N+1)$ and $P_k(N-1)$ are the natural populations for the atom k in the neutral, anionic and cationic species respectively.

## 3. Results and Discussion

*3.1. Weight loss measurements*

*3.1.1. Effect of inhibitor concentration*

The inhibition efficiency values for mild steel in 1.0 M HCl media at different concentrations of the inhibitor are presented in Table 1. It is apparent that the inhibition efficiency increased with the increase in inhibitor concentration in 1.0 M HCl media. This behavior can be explained based on strong interaction of the inhibitor molecule with the metal surface resulting in adsorption [26]. The extent of adsorption increases with the

increase in concentration of the inhibitor leading to increased inhibition efficiency. In the acid solutions, the maxi-mum inhibition efficiency was observed at an inhibitor concentration of $10^{-3}$M. Generally, organic inhibitors suppress the metal dissolution by forming a protective film adsorbed to the metal surface and separating it from the corrosion medium [27-28].The high inhibition efficiency of P2 is attributed due to large molecular size, the presence of severalaromatic rings and heteroatoms (S, O) which influenced the adsorption of the drug on mild steel surface.

**Table 1:**Impedance parameters with corresponding inhibition efficiency for the corrosion of mild steel in 1.0 M HCl at different concentrations of (**P2**).

| **Inhibitor** | **Concentration** (M) | ***v*** ($mg.cm^{-2}\,h^{-1}$) | $\mathbf{E_w}$ (%) |
|---|---|---|---|
| **1M HCl** | -- | 0.82 | -- |
| **P2** | $\mathbf{10^{-6}}$ | 0.34 | 59 |
| | $\mathbf{10^{-5}}$ | 0.21 | 74 |
| | $\mathbf{10^{-4}}$ | 0.13 | 84 |
| | $\mathbf{10^{-3}}$ | 0.09 | 89 |

*3.1.2. Adsorption isotherm*

The adsorption of organic compounds on metal surface is explained by the substitution of water molecules which facilitate the access of hydrogen ions to the surface and then the corrosion attack. This replacement may cover the metal surface and then reduces the surface area that is available for the attack of the aggressive ion from the acid solution. The corrosion rate decreases with increase with the inhibitor concentration.
In our present study, in order to clarify the nature and strength of adsorption, Langmuir, Temkin and Frumkin isotherms were tested. As can be seen from figure 1 adsorption of P2obeys the Longmuir isotherm given by equation:

$$\frac{\theta}{1-\theta} = C_{inh} \,.\, K_{ads} \qquad \textbf{(12)}$$

Where $K_{ads}$ is the equilibrium constant of adsorption adsorption/desorption process, θ isSurface covered and C is the inhibitor concentration.

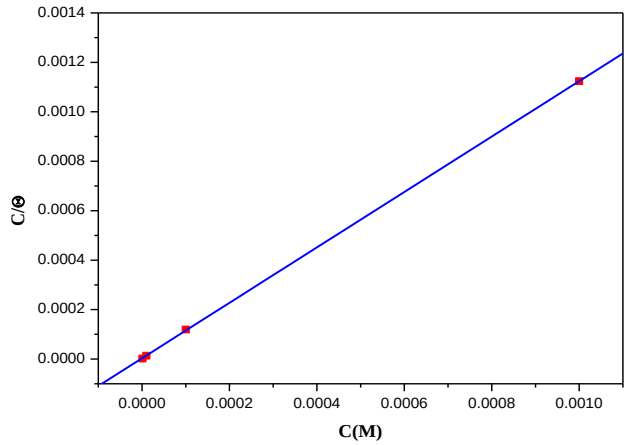


**Figure 1:** Langmuir isotherm for the adsorption of P2 on the mild steel surface.

The behavior of equilibriumconstants obtained from Langmuir model was similarto the values which obtained by kinetic–thermodynamicmodel. The standard free energy of adsorption ($\Delta G_{ads}$), is related to the $K_{ads}$ by the equation [29]:

$$\Delta G_{ads} = -RT\ln(55{,}5K) \qquad \textbf{(13)}$$

Where R is the universal gas constant and T is the absolute temperature.

The calculated value of free energy of adsorption was found to be $\Delta G°_{ads}$= −42.49 kJ $mol^{-1}$, where adsorption–desorption equilibrium constant *K* value was obtained from the linear regression of Langmuir isotherm ($3.17x10^5$L $mol^{-1}$).The negative value of $\Delta G°_{ads}$ indicates that the inhibitor, in this case P2 is spontaneously adsorbed onto the mild steel surface. It is well known that values of $\Delta G°_{ads}$ around −20 kJ $mol^{-1}$ or lower are associated with the physisorption phenomenon where the electrostatic interaction assemble between the charged molecule and the charged metal, while those around −40 kJ $mol^{-1}$or higher are associated with the chemisorption phenomenon where the sharing or transfer of organic molecules charge with the metal surface occurs [30, 31].
The calculated value of $\Delta G°_{ads}$ is negative. The increasingly negative adsorption free energy ($\Delta G°_{ads}$) reflects the spontaneity of the adsorption of the inhibitor molecules and more $\Delta G°_{ads}$ is negative and more the adsorbed layer on steel surface is stable.

*3.2. Potentiodynamic polarization measurements*

The potentiodynamic polarization nature of P2 on mild steel corrosion in 1M HCl is shown in Fig. 2 and polarization parameters such as corrosion potential ($E_{corr}$), corrosion current density ($I_{corr}$), anodic and cathodic Tafel slopes ($\beta_c$; $\beta_a$) and corresponding inhibition efficiency (E%) were calculated from extrapolation of linear segments of the anodic and cathodic Tafel curves and given in Table 2.

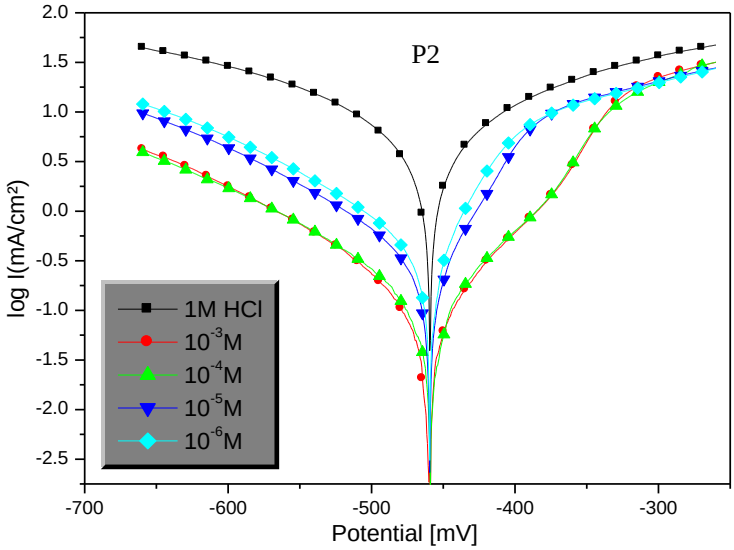


**Figure 2:** Polarisation curves of mild steel in 1M HCl at different concentrations of P2.

**Table 2:** Values of electrochemical parameters evaluated from the cathodic current-voltage characteristics for the system electrode/1 M HCl with and without added inhibitor at 308 K.

| Inhibitor | **Concentration** (M) | **Ecorr** (mV/SCE) | **Icorr** (µA/$cm^2$) | **-βc** (V/dec) | **βa** (V/dec) | **$E_p$** (%) |
|---|---|---|---|---|---|---|
| **HCl 1M** | -- | -459 | 1381 | 299 | 174 | -- |
| **P2** | **$10^{-6}$** | -455 | 647 | 273 | 180 | 53 |
| | **$10^{-5}$** | -458 | 441 | 284 | 177 | 68 |
| | **$10^{-4}$** | -457 | 293 | 258 | 192 | 79 |
| | **$10^{-3}$** | -461 | 162 | 269 | 101 | 88 |

From the results depicted in Table 2it can be seen that values of corrosion current density (icorr) for mild steel in 1M HCl decreased with increase in P2 concentration. This decrease in $i_{corr}$ values might be attributed due to adsorption of the P2 at metal/electrolyte interfaces and therefore, it can be concluded that P2 inhibits mild steel corrosion by adsorbing on the mild steel surface which isolates the metal from aggressive acid solution [32, 33]. Moreover, the maximum shift in the value of Ecorr in the present study was 3 mV which is less than 85 mV. Therefore, the P2 can be classified as mixed-type inhibitor, which implies the inhibitor reduces the anodic mild steel dissolution and also retards the cathodic hydrogen evolution reaction [34, 35]. Moreover, from the results depicted in Table 2it can be observed that in the presence of P2 at different concentrations the values of βa change as compared to in free acid solution. However, the shifts in values of βc were more prominent as compared to shift in βa suggesting that P2 acts as predominantly cathodic type inhibitor [36, 37].

### *3.3. Electrochemical impedance spectroscopy (EIS)*

Fig. 3 represents the Nyquist plots for mild steel corrosion in the absence and presence of different concentrations of P2 after 30 min immersion time. It can be seen from the figure that Nyquist plots consist of single semicircle capacitive loop which corresponds to one time constant in Bode plots (Fig. 4). This finding suggests that corrosion of mild steel in 1M HCl is mainly controlled by a charge transfer process [38].

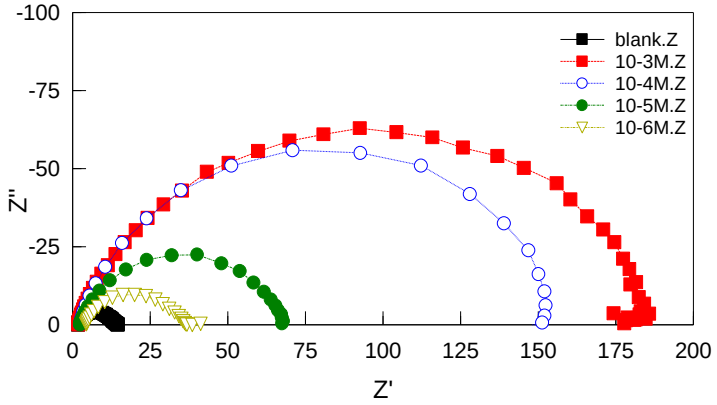


**Figure 3:** Nyquist diagram for mild steel in 1 M HCl in the absence and presence of P2.

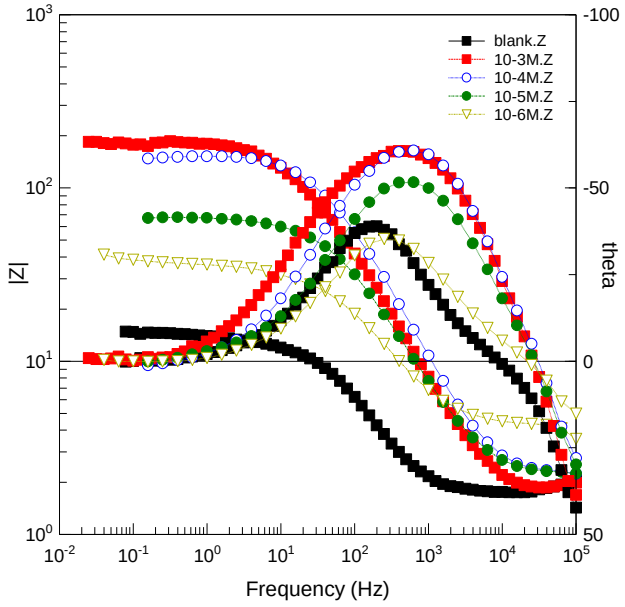


**Figure 4:** Bode and phase plots of mild steel in 1.0 M HCl and in the presence different concentrations of P2 at 308 K.

Some common impedance parameters such as solution resistance (Rs), charge transfer resistance ($R_{ct}$), double layer capacitance ($C_{dl}$), surface coverage (θ) and inhibition efficiency (E%) were calculated using equivalent circuit model described elsewhere [39] and given in Table 3.

**Table 3:** Electrochemical parameters for mild steel in 1 M HCl without and with different concentrations of **(**P2**)** at 308K.

| Concentration (M) / Prameters | **1M HCl** | **$10^{-6}$** | **$10^{-5}$** | **$10^{-4}$** | **$10^{-3}$** |
|---|---|---|---|---|---|
| Real Center | 9.25 | 20.691 | 35.126 | 77.963 | 93.155 |
| Imag. Center | 1.62 | 10.712 | 12.636 | 20.26 | 33.761 |
| Diameter | 15.13 | 39.934 | 70.509 | 155.93 | 194.57 |
| Deviation | 0.15 | 0.90454 | 0.29383 | 1.9786 | 2.1196 |
| Low Intercept $R_s$ ($\Omega.cm^2$) | 1.86 | 3.8397 | 2.214 | 2.6755 | 1.9154 |
| High Intercept $R_t$ ($\Omega.cm^2$) | 16.64 | 37.541 | 68.039 | 153.25 | 184.4 |
| Depression Angle | 12.42 | 32.443 | 21.003 | 15.061 | 20.306 |
| $\omega_{max}$ ( rad $s^{-1}$) | 929.60 | 364.98 | 332.97 | 213.12 | 98.289 |
| Estimated $R_t$($\Omega.cm^2$) | 14.78 | 33.702 | 65.825 | 150.58 | 182.48 |
| Estimated $C_{dl}$($F.cm^{-2}$) | 7.11 E-5 | 6.861E-5 | 4.2594E-5 | 3.0092E-5 | 2.2289E-5 |
| $\mathbf{E_R}$(%) | -- | 56 | 78 | 90 | **92** |

Inspection of the results shown in Table 3 suggests that values of $C_{dl}$ decreased and values of $R_{ct}$ increased in the presence of the P2. Furthermore, this decrease in $C_{dl}$ and increase in $R_{ct}$ values are more pronounced at higher P2 concentrations.
The decreased value of $C_{dl}$ in the presence of P2 is due to the decrease in local dielectric constant and/or an increase in the thickness of the electrical double layer [40, 41]. The increase in $R_{ct}$ values in the presence of P2 is credited due to formation of protective film at the metal/solution interface by P2 [42, 43]. This finding suggests that P2 inhibits mild steel corrosion in 1M HCl by protective surface film at metal/electrolyte interfaces.

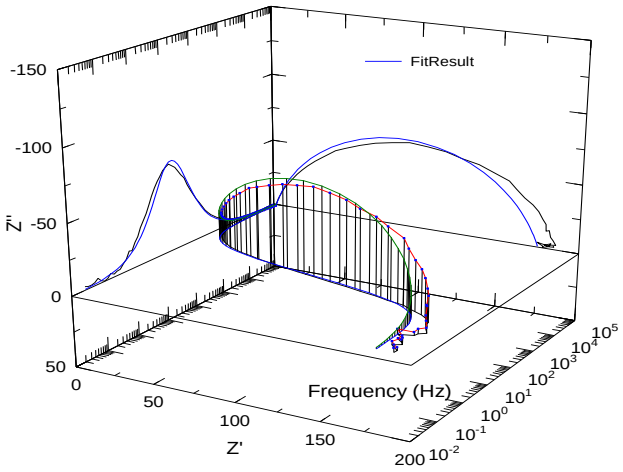


**Figure 5:** EIS Nyquist and Bode diagrams 3D for mild steel / 1 M HCl + $10^{-3}$ M of **P2** interface: (----) experimental; (------) fitted data.

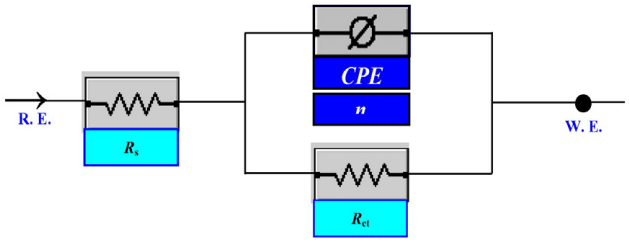


**Figure 6:** Equivalent circuit model used to fit the impedance spectra.

An equivalent circuit was introduced to explain the EIS data as shown in Fig. 6.This circuit is generally used to describe the iron/acid interface model [44]. In this circuit Rs solution resistance, $R_{ct}$ charge transfer resistance, and CPE is a constant phase element.

*3.3. Computational theoretical studies*

The FMOs (HOMO and LUMO) are very important for describing chemical reactivity. The HOMO containing electrons, represents the ability ($E_{HOMO}$) to donate an electron, whereas, LUMO haven't not electrons, as an electron acceptor represents the ability ($E_{LUMO}$) to obtain an electron. The energy gap between HOMO and LUMO determines the kinetic stability, chemical reactivity, optical polarizability and chemical hardness–softness of a compound [45]. Firstly, in this study, we calculated the HOMO and LUMO orbital energies by using B3LYP method with 6-31G which is implemented in Gaussian 09 packadge [46; 47]. All other calculations were performed using the results with some assumptions. The higher values of $E_{HOMO}$ indicate an increase for the electron donor and this means a better inhibitory activity with increasing adsorption of the inhibitor on a metal surface, where as $E_{LUMO}$ indicates the ability to accept electron of the molecule. The adsorption ability of the inhibitor to the metal surface increases with increasing of $E_{HOMO}$ and decreasing of $E_{LUMO}$. The HOMO and LUMO orbital energies of the P2 inhibitors were performed and were shown in Table 4 and Figure 7. High ionization energy (> 6 eV) indicates high stability of P2 inhibitor [48], the number of electrons transferred (ΔN), dipole moment, Ionisation potential**,** electron affinity, electronegativity, hardness, Softness and total energy were also calculated and tabulated in Table 4.

**Table 4.** Quantum chemical parameters for P2 obtained in gas and aqueous phase with the DFT at the B3LYP/6-31G level.

| **Prameters** | **Gas phase** | **Aqueous phase** |
|---|---|---|
| Total Energy *TE* (eV) | -65688.4 | -65688.8 |
| $E_{HOMO}$ (eV) | -5.6662 | -6.1726 |
| $E_{LUMO}$ (eV) | -1.0492 | -2.7784 |
| Gap $\Delta E$ (eV) | 4.6170 | 3.3942 |
| Dipole moment $\mu$ (Debye) | 6.8470 | 9.4567 |
| Ionisation potential $I$ (eV) | 5.6662 | 6.1726 |
| Electron affinity $A$ | 1.0492 | 2.7784 |
| Electronegativity $\chi$ | 3.3577 | 4.4755 |
| Hardness $\eta$ | 2.3085 | 1.6971 |
| Electrophilicity index $\omega$ | 2.4419 | 5.9013 |
| Softness $\sigma$ | 0.4332 | 0.5892 |
| Fractions of electron transferred | 0.7889 | 0.7438 |

The value of ΔN (number of electrons transferred) show that the inhibition efficiency resulting from electron donation agrees with Lukovit's study [49]. If $\Delta N < 3.6$, the inhibition efficiency increases by increasing electron donation ability of these inhibitors to donate electrons to the metal surface [50].

Pertinent valence and dihedral angles, in degree, of the studied inhibitor calculated at B3LYP/6-31G(d,p) in gas and aqueous phases are given in the table 5.

Table 5 displays the most relevant values of the natural population (P(N), P(N-1) and P(N+1)) with the corresponding values of the Fukui functions ($f_k^+$ and $f_k$) of the studied inhibitors. The calculated values of the $f_k^+$ for inhibitors are mostly localized on the 4,5-bis(hydroxymethylthio)-1,3-dithiolane-2-thione ring, namely $C_1$, $S_4$, $S_5$ and $S_6$, indicating that the 4,5-bis(hydroxymethylthio)-1,3-dithiolane-2-thione ring will probably be the favorite site for nucleophilic attacks.

The geometry of P2 in gas and aqueous phase (Fig. 7) were fully optimized using DFT based on Beck's three parameter exchange functional and Lee–Yang–Parr nonlocal correlation functional (B3LYP) [51-54] and the 6–31G. The optimized structure shows that the molecule P1 have a non-planar structure.The HOMO and LUMO electrons density distributions of P2are given in Table 6.

As we know, frontier orbital theory is useful in predicting the adsorption centres of the inhibitors responsible for the interaction with surface metal atoms. Table 6 show the HOMO and LUMO orbital contributions forthe neutral studied inhibitor. The HOMO densities were concentrated on isatine ring.

**Table 5.** Pertinent valence and dihedral angles, in degree, of the studied inhibitors calculated at B3LYP/6-31G(d,p) in gas, G and aqueous, A phases

| Angle | phase | value |
|---|---|---|
| $[C_9C_{12}O_{15}]$ | G | 108.9 |
| | A | 108.9 |
| $[C_2S_8C_{17}]$ | G | 99.4 |
| | A | 100.0 |
| $[S_7C_9C_{12}O_{15}]$ | G | -67.9 |
| | A | -68.3 |
| $[S_8C_2C_3S_7]$ | G | 3.5 |
| | A | 4.2 |

**Table 6.** *Fukui functions of P2 calculated at B3LYP/6-31G in gas and aqueous phases.*

| | Gas | | aqueous | |
|---|---|---|---|---|
| | F- | f+ | F- | f+ |
| C 1 | 0.1146 | -0.0560 | 0.1255 | -0.0425 |
| C 2 | 0.0045 | 0.0506 | 0.0028 | 0.0609 |
| C 3 | 0.0088 | 0.0178 | 0.0024 | 0.0238 |
| S 4 | 0.3546 | 0.3241 | 0.3838 | 0.3350 |
| S 5 | 0.1674 | 0.1275 | 0.1861 | 0.1317 |
| S 6 | 0.1473 | 0.1603 | 0.1886 | 0.1699 |
| S 7 | 0.0603 | 0.1563 | 0.0392 | 0.1640 |
| S 8 | 0.0488 | 0.0720 | 0.0334 | 0.0586 |
| C 9 | 0.0035 | -0.0013 | 0.0007 | -0.0026 |
| H 10 | -0.0031 | 0.0083 | 0.0023 | 0.0114 |
| H 11 | 0.0231 | 0.0255 | 0.0080 | 0.0151 |
| C 12 | -0.0053 | -0.0061 | -0.0012 | -0.0024 |
| H 13 | 0.0208 | 0.0300 | 0.0051 | 0.0164 |
| H 14 | 0.0132 | 0.0139 | 0.0040 | 0.0091 |
| O 15 | -0.0164 | -0.0125 | -0.0021 | -0.0001 |
| H 16 | 0.0134 | 0.0162 | 0.0032 | 0.0070 |
| C 17 | 0.0034 | 0.0071 | 0.0005 | 0.0058 |
| H 18 | 0.0011 | 0.0025 | 0.0029 | 0.0052 |
| H 19 | 0.0050 | 0.0138 | 0.0051 | 0.0115 |
| C 20 | -0.0041 | -0.0056 | -0.0010 | -0.0016 |
| H 21 | 0.0081 | 0.0094 | 0.0030 | 0.0059 |
| H 22 | 0.0182 | 0.0243 | 0.0047 | 0.0102 |
| O 23 | 0.0077 | 0.0142 | 0.0015 | 0.0051 |
| H 24 | 0.0050 | 0.0077 | 0.0013 | 0.0028 |

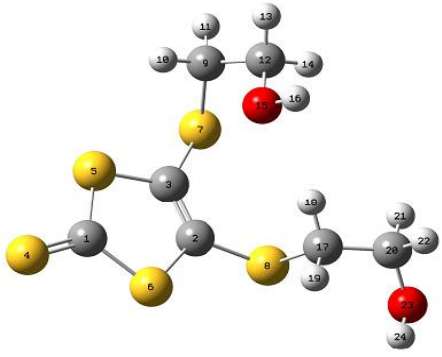

**Figure 7**. Optimized molecular structures in gas phase with the DFT at the B3LYP/6-31G level

## Conclusion

From the above study it can be concluded that 4, 5- (alkylthio) - 1, 3- dithiole- 2- thione (P2) acts as good corrosion inhibitor. The corrosion inhibition efficiency increases with increasing P2 concentration. Adsorption of the P2on the mild steel surface obeyed the Langmuir isotherm. Polarization study revealed that P2 acted as mixed type but predominantly cathodic inhibitor. EIS studies revealed that the studied drug formed a protective surface film at metal/electrolyte interfaces. The calculated quantum chemical parameters are supports the obtained E (%) of the inhibitor.

## Reference

1. Böttcher B., Lüttringhaus, Liebigs A., *Ann. Chem*. 557(1947)89.
2. Yamada J., Sugimoto T., *TTF Chemistry Fundamentals and Applications of Tetrathiafulvalene, Springer, Berlin*, (2004).
3. Bryce M. R., *J. Mater. Chem*. 10(2000)589.
4. Wang C., Chen Q., Sun F., Zhang D., Zhang G., Huang Y., Zhao R., Zhu D., *J. Am. Chem. Soc*.132 (2010) 3092.
5. Jia H.P., Liu S.X., Sanguinet L., Levillain E., Decurtins S., *J. Org. Chem.*74 (2009) 5727.
6. Nguyen T. L. A., Devic T., Mialane P., Rivière E., Sonnauer A., Stock N., Demir-Cakan R., Morcrette M., Livage C., Marrot J., Tarascon J.M., Férey G., *Inorg Chem*. 49 (2010) 10710.
7. Ferraris J., Cowan D.O., Walatka V., Perlstein J.H., *J Am Chem Soc*. 95 (1973) 948.
8. Hasegawa M., Sone Y., Iwata S., Matsuzawa H., Mazaki Y., *Org Lett*. 13 (2011) 4688.
9. Nakamura K., Takashima T., Shirahata T., Hino S., Hasegawa M., Mazaki Y., Misaki Y., *Org Lett*. 13 (2011) 3122.
10. Takase M., Yoshida N., Nishinaga T., Iyoda M., *Org Lett*. 13 (2011) 3896.
11. Chen G., Mahmud I., Dawe L.N., Daniels L.M., Zhao Y., *J Org Chem*. 76 (2011) 2701.
12. Canevet D., Sallé M., Zhang G., Zhang D., Zhu D., *Chem Commun*. 17 (2009) 2245.
13. Batail P., *Chem Rev*. 104 (2004) 4887.
14. Coskun A., Spruell J.M., Barin G., Fahrenbach A.C., Forgan R.S., Colvin M.T., Carmieli R., Benítez D., Tkatchouk E., Friedman D.C., Sarjeant A.A., Wasielewski M.R., Goddard W.A., Stoddart J.F., *J Am ChemSoc*. 133 (2011) 4538.
15. Klajn R., Stoddart J F., Grzybowski B.A, *Chem. Soc Rev*. 39 (2010) 2203.
16. Bryce M.R., *J Mater Chem*. 10 (2000) 589.
17. Nielsen M.B., Lomholt C., *J. Chem. Soc. Rev*. 29 (2000) 153.
18. Segura J.L., Martín N., *Angew Chem Int Ed*. 40 (2001) 1372.
19. Otsubo T., Takimiya K., *Bull Chem Soc Japan*. 1 (2004) 43.
20. Bryce M.R., *Adv Mater*. 11 (1999) 11.
21. Elmsellem H., Basbas N., Chetouani A., Aouniti A., Radi S., Messali M., Hammouti B., *Portugaliae Electrochimica. Acta*. 2 (2014) 77.
22. Bentiss F., Gassama F., Barbry D., Gengembre L., Vezin H., Lagrenee M., Traisnel M., *Appl. Surf. Sci.* 252 (2006) 2 684.
23. Zerga B., Hammouti B., Ebn Touhami M., Touir R., Taleb M., Sfaira M., Bennajeh M., Forssal I., *Int J. Electrochem. Sci.* 7(2012)471 – 483.
24. Quraishi M.A., Sharma H.K., *Chem. Phys*. 78 (2002) 18.
25. Quraishi M.A., Sardar R., Jamal D., *Mater. Chem. Phys*. 71(2001) 309.
26. Elmsellem H., Youssouf M. H., Aouniti A., Ben Hadd T., Chetouani A., Hammouti B., *Russian, Journal of Applied Chemistry*. 87(6) (2014) 744.
27. Kustu C., Emregul K.C., Atakol O., *Corros. Sci*. 49(2007)2800.
28. Singh A K., Quraishi M.A. *J. Mater. Environ. Sci.* 1(2010)101.
29. Elmsellem H., Nacer H., Halaimia F., Aouniti A., Lakehal I., Chetouani A., Al-Deyab S. S., Warad I., Touzani R., Hammouti B,.*Int. J. Electrochem. Sci*. 9(2014)5328.
30. Elmsellem H., AounitiA., Youssoufi M.H., BendahaH., Ben hadda T., Chetouani A., Warad I., Hammouti B., *Phys. Chem. News*.70(2013)84.
31. Elmsellem H., Harit T., AounitiA., Malek F., Riahi A., Chetouani A., Hammouti B., *Protection of Metals and Physical. Chemistry of Surfaces.* 5(2015)873.
32. Govindarajan M., Karabacak M., *Spectrochim Acta Part A Mol Biomol Spectrosc*, 85 (2012)251-60.

33. Becke A.D., *J. Chem. Phys*. 98(1993)1372.
34. Filali Baba Y., Elmsellem H., Kandri Rodi Y., Steli H., AD C., Ouzidan Y., Ouazzani Chahdi F., Sebbar N. K., Essassi E. M., and Hammouti B., *Der Pharma Chemica*, 8(2016)159-169.
35. Elmsellem H., Karrouchi K., Aouniti A., Hammouti B., Radi S., Taoufik J., Ansar M., Dahmani M., Steli H. and El Mahi B., *Der Pharma Chemica*, 7(2015)237-245.
36. Lukovits I., Kalman E., Zucchi F., *Corrosion*, 57(2001)3-7.
37. Sikine M., Kandri Rodi Y., Elmsellem H., Krim O., Steli H., Ouzidan Y., Kandri Rodi A., Ouazzani Chahdi F., Sebbar N. K., Essassi E. M., *J. Mater. Environ. Sci*, 7(2016)1386-1395.
38. Hjouji M. Y., Djedid M., Elmsellem H., Kandri Rodi Y., Ouzidan Y., Ouazzani Chahdi F., Sebbar N. K., Essassi E. M., Abdel-Rahman I., Hammouti B., *J. Mater. Environ. Sci*, 7(2016)1425-1435.
39. Lee C., Yang W., Parr R.G., *Phys. Rev*. B,37(1988)785.
40. Chakib I., Elmsellem H., Sebbar N. K., Lahmidi S., Nadeem A., Essassi E. M., Ouzidan Y., Abdel-Rahman I., Bentiss F., Hammouti B., *J. Mater. Environ. Sci.* 7(2016)1866-1881.
41. Bentiss F., Jama C., Mernari B., El Attari H., El Kadi L., Lebrini M., Traisnel M., Lagrenée M., *Corros. Sci*. 51 (2009) 1628.
42. Zerga B., Hammouti B., Ebn Touhami M., Touir R., Taleb M., Sfaira M., Bennajeh M., ForssalInt I., *J. Electrochem. Sci.* 7(2012)471 – 483.
43. Quraishi M.A., SardarR., *Mater. Chem. Phys*. 78 (2002) 425.
44. Elmsellem H., Aouniti A., Khoutoul M., Chetouani A., Hammouti B., Benchat N., Touzani R., Elazzouzi M., *J. Chem. Pharm. Res*. 6 (2014) 1216.
45. Govindarajan M., Karabacak M., *Spectrochim Acta Part A Mol Biomol Spectrosc*, 85 (2012)25.
46. Becke A.D., *J. Chem. Phys*. 98 (1993) 1372.
47. Filali Baba Y., Elmsellem H., Kandri Rodi Y., Steli H., AD C., Ouzidan Y., Ouazzani Chahdi F., Sebbar N. K., Essassi E. M., and Hammouti B., *Der Pharma Chemica*. 8 (2016) 159-169.
48. Ellouz M., Elmsellem H., Sebbar N. K., Steli H., Al Mamari K., Nadeem A., Ouzidan Y., Essassi E. M., Abdel-Rahaman I., Hristov P., *J. Mater. Environ. Sci*. 7(7) (2016) 2482-2497
49. Lukovits I., Kalman E., Zucchi F., *Corrosion*, 57 (2001) 3-7.
50. Sikine M., Kandri Rodi Y., Elmsellem H., Krim O., Steli H., Ouzidan Y., Kandri Rodi A., Ouazzani Chahdi F., Sebbar N. K., Essassi E. M., *J. Mater. Environ. Sci*, 7 (4) (2016) 1386-1395
51. Hjouji M. Y., Djedid M., Elmsellem H., Kandri Rodi Y., Ouzidan Y., Ouazzani Chahdi F., Sebbar N. K., Essassi E. M., Abdel-Rahman I., Hammouti B., *J. Mater. Environ. Sci*, 7 (4) (2016) 1425-1435.
52. Lee C., Yang W., Parr R.G., *Phys. Rev. B.* 37 (1988) 785
53. El Azzouzi M., Aouniti A., Tighadouin S., Elmsellem H., Radi S., Hammouti B., El Assyry A., Bentiss F., Zarrouk A., J. Moll. Liq. 221 (2016) 633-641 (2016).DOI: 10.1016/j.molliq.2016.06.007
54. Elmsellem H., Elyoussfi A., Sebbar N. K., Dafali A., Cherrak K., Steli H., Essassi E. M., Aouniti A. and Hammouti B., *Maghr. J. Pure & Appl. Sci*.1 (2015) 1-10.